Synchronize cells in the cell cycle phases to correlate with their heterogeneous biomechanical properties

Valentin Fonvieille, Ophélie Thomas- -Chemin, Etienne Dague

FONVIEILLE Valentin

Synchronize cells in the cell cycle phases to correlate with their heterogeneous biomechanical properties

Supervisor: Ophélie THOMAS-CHEMIN

Director: Etienne DAGUE

ELiA team, LAAS-CNRS, Toulouse

2022-2023

Summary:

Abstract

The study of cells' mechanical properties is crucial for understanding their behavior and the development of diseases. This report focuses on the methods allowing the characterization of the mechanical properties of non-cancerous (RWPE-1) and cancerous (PC3-GFP) prostate cell lines, through the cell cycle. The goal is to investigate the impact of different cell cycle phases on the cells' mechanics.

Atomic Force Microscopy (AFM) is used to measure the mechanical properties by analyzing the force-distance curves obtained from the interaction between a cantilever and the cell surface. Previous work using unsupervised machine learning identified subgroups with distinct mechanical characteristics within a same cell population. It is hypothesized that changes in the mechanical properties of cells are related to the cell cycle phases, as the cytoskeleton, which determines cell mechanics, undergoes dynamic changes during the cell cycle. The report describes the experimental procedures, including cell synchronization using serum deprivation, flow cytometry control, comparing cell distribution in the cell cycle phases with subclasses proportions, and future experiments involving Fluorescent Ubiquitination-based Cell Cycle Indicator (FUCCI) cells.

Results show that serum deprivation did not effectively synchronize the RWPE-1 and PC3-GFP cells, but the mechanical subclasses obtained from previous work exhibit differences in distribution that may correspond to different cell cycle phases. The report discusses possible reasons for the lack of synchronization and suggests alternative methods. Additionally, it highlights the need for improved analysis techniques to better correlate the mechanical subclasses with the cell cycle distribution. Overall, this research contributes to understanding the relationship between cell mechanics and the cell cycle, which can lead to advancements in diagnosing and treating diseases.

I. Introduction

The study of the cells' mechanical properties is a growing field of research that aims to understand how cells interact with their physical environment. Cells are subjected to a variety of mechanical forces in their microenvironment, including when they deform, migrate, divide, and interact with each other or with the extracellular matrix.

The cells' mechanical properties such as their stiffness, elasticity, adhesion and response to mechanical forces, play a key role in their behavior and cell fate. Studying these mechanical properties can lead to a better understanding of normal cell physiology, as well as diseases that result from mechanical cell dysfunction. For example, progeria or muscular dystrophy are directly the consequence of cellular mechanical problems due to mutations affecting proteins from the cytoskeleton (Ahmed *et al.* 2018; Pandey *et al.* 2015). Moreover, in a cancer context, cell mechanics can influence the tumor invasiveness and promote metastasis (Smolyakov *et al.* 2016).
By studying the mechanical properties of cells, it will be possible to develop new approaches to diagnose, treat and prevent these diseases, paving the way for significant advances in biology and medicine.

Several techniques can be used to study the cells' mechanical properties (Wu *et al.* 2018). Atomic Force Microscopy (AFM) consists in studying the mechanical behavior of biological materials. Contrary to other techniques, measurement techniques involving Atomic Force Microscopy (AFM) probes the cell locally, on adherent cells, can be coupled with a microscope (fluorescent or not), and uses different shapes of tips to probe different organelles of the cell.

The AFM measures a force between a cantilever and a sample. The cantilever approaches and retracts from the sample surface and is attracted or repelled by the sample. This is the deflection of the cantilever. This deflection is measured with a laser that reflects off the back of the cantilever and is sent back to a 4 quadrants photodiode (schema 1). The approach and retract of the tip form the force-distance curves (schema 2). From these force measurements, the mechanical properties of the sample are calculated.

By analyzing the mechanical properties of these curves by machine learning in the previous work of my team, 3 and 4 sub-groups, among healthy prostate cells (RWPE-1) and cancerous prostate cells (PC3) have been identified, respectively. These subclasses among the population present different mechanical characteristics. In this way, since the PC3-GFP cell line has more subclasses than the RWPE-1 cell line, it can be said to be more heterogeneous, which could be due to its cancerous character. One of the hypotheses that follows from these results is that the cell changes its mechanical properties according to the phase of the cell cycle. Indeed, the cell owes almost all its mechanical properties to its cytoskeleton (Pegoraro *et al.* 2017). It is composed of 3 protein structures (microfilaments, microtubules and intermediate filaments), and their dynamic is involved in the dividing process, contractility, shape, adhesion, rigidity, elasticity of the cells. These dynamics change during the cell cycle, and by consequence, the mechanics too.

The objective of this work is to characterize the different phases of the cell cycle in non-cancerous and cancerous cell populations. Following single-cell AFM acquisitions, this will help address the question: Do the different cell cycle phases influence cellular mechanics?

II. Materials and methods

1. Samples

The following experiments were performed on two different cell lines from prostate:

RWPE-1 cells, which is a non-cancerous prostate cell line; and PC3-GFP cells, which is a cancerous cell line isolated from prostatic adenocarcinoma metastatic, expressing GFP.

2. Cell synchronization using serum deprivation

. Sample preparation

The RWPE-1 cell line (ATCC CRL-11609) was cultured in K-SFM medium with 0.05 mg/mL Bovine Pituitary Extract (BPE), 5 ng/mL Epidermal Growth Factor (EGF) and 1 % penicillin-streptomycin (Gibco™, Thermo Fisher Scientific Inc.). The flask was incubated at 37 °C and 5 % CO_2 to reach 70/80 % confluence. Then, the culture medium was changed, with a K-SFM medium without Bovine Pituitary Extract and Epidermal Growth Factor. Cells

were incubated in serum deprivation condition for 24 hours in a 37 °C incubator and 5 % CO_2.

The control flask was cultured in the same way, but the Bovine Pituitary Extract and Epidermal Growth Factor did not have been removed from the medium.

The PC3-GFP cell line was cultured in RPMI medium, containing L-glutamine, HEPES buffer and phenol red (Gibco™, Thermo Fisher Scientific Inc.), 1 % penicillin-streptomycin (Gibco™, Thermo Fisher Scientific Inc.) and 1 % geneticin (G418, Gibco™, Thermo Fisher Scientific Inc.), with or without 10 % fetal bovine serum (SVF, Gibco™, Thermo Fisher Scientific Inc.). The tumorous cell line PC3- GFP, was grown at 37 °C with 5 % CO_2.

b. Flow cytometry control

For each of the two conditions, cells were treated with trypsin EDTA to suspend them. Cells were centrifuged at 1300 rpm for 5 minutes, supernatant was discarded. Cells were counted and split equally in 4 cytometry tubes, in 150 µL PBS for each tube. Cells were fixed with 350 µL ethanol 100 %. Cells were incubated for 2 hours at -4 °C. They were centrifuged two times and washed with PBS. There are 4 solutions per tube, both for control condition and serum deprivation. Cells are incubated 15 minutes in the dark in 6 µL Propidium Iodide, 2µL of KI antibody and QSP for 200 µL for the first tube; only 6 µL Propidium Iodide and QSP for 200 µL PBS for the second tube; only 2 µL KI antibody and QSP for 200 µL PBS for the third tube; and 200 µL of PBS for the last tube. Cells were analyzed by FACS. Compensation and calibration parameters are the same for every analysis.

3. Fluorescent Ubiquitination-based Cell Cycle Indicator (FUCCI) cells, an alternative to cell synchronization

These experiments have not yet been conducted due to time constraints. However, the bibliographical research, protocol study, and ordering of necessary materials (bacteria containing the plasmid, miniprep kit, primers, and lipofectamine) were completed. This groundwork will enable the team to proceed with its research using the following methods.

The FUCCI system is developed by creating fusion proteins in plasmid. These chimeric proteins are composed of finely regulated proteins across the cell cycle, and a fluorescent protein. Here, the CDT1 protein is fused with the fluorescent mKO2 (monomeric Kusabira-Orange2) protein

and the Geminin protein is fused with the mAG1 (monomeric Azami-Green1) protein. Both chimeric proteins are under the expression of the ubiquitous EF1α promoter. In addition, ampicillin and puromycin resistance cassettes were integrated to the plasmid.

The CDT1 protein was chosen because it is only expressed in the G1 and early S phases of the cell cycle. In addition, the Geminin protein is absent during the G1 phase, but it is only expressed during the S/G2/M phases. Thus, we will be able to follow the cell cycle of cells integrating the plasmid system pBOB-EF1-FastFUCCI-Puro (schema 3) into our cell lines.

a. DNA purification

Plasmid is contained in *Escherichia coli* bacteria. These bacteria are transferred on a Petri dish containing agar plate, and ampicillin to cultivate bacteria which have conserved the plasmid. The Petri dish is incubated at 37 °C overnight. The next day, only one colony is picked from the Petri dish (to avoid the presence of mutated bacteria), and is inoculated in liquid culture medium LB in a tube. The culture tube is incubated at 37 °C overnight, to increase the number of bacteria, and therefore the plasmid copy number.

Plasmid DNA purification is performed following the Plasmid Miniprep Kit protocol from ThermoFisher (Invitrogen™-Kit Miniprep for plasmids PureLink™ HiPure). A plasmid purified solution is obtained.

b. Plasmid control

In order to control the absence of mutation in the plasmid construct, we have to sequence our zone of interest, with specific primers. The sequencing zone is composed of the recombinant proteins and measures almost 2000 bp. The sequencing is reliable until almost 800 bp, so we need to design 3 pairs of primers overlapping shown on the schema 4.

c. Cell Transfection

The plasmid purified solution must be mixed with lipofectamine (lipofection reagent). The mix rests for 5 minutes at room temperature to allow the formation of lipo complexes containing plasmids.

RWPE-1 and PC3 cultures will be transfected with the lipo complex solution. The cell lines will be incubated for 72 hours in a 37 °C incubator and 5 % CO_2 in their respective culture medium,

containing 10 % serum. Then, transfected cells containing plasmid will be selected with puromycin at a given concentration to select the cells which will integrate the plasmid only.

d. Acquisition with AFM: Calibration of the cantilevers: sensitivity and spring constant

All AFM experiments are performed on a NanoWizard® III AFM device (JPK Instruments, Bruker Nano GmbH.) in contact mode, force mapping. Before any experiment, the sensitivity of the AFM photodiode is calibrated. In this study, colloidal-shaped cantilevers with a sensitivity of 33.49 nm/V to 46.64 nm/V. The spring constant was then calibrated by studying the thermal fluctuation of the cantilever at 37 °C. The peak of the thermal spectrum was fitted to extract the resonant frequency. In this study, the colloidal cantilevers had spring constants ranging from 0.016 N/m and 0.031 N/m. Force mapping measurements were performed in culture medium buffered with 5 % CO_2 and maintained at 37 °C using a PetriDishHeater (Bruker). Mapping was done with a relative setpoint of 3 nN, Z length of 5 µm, extension velocity of 50 µm/s, and in 4x4 pixels over 10x10 µm² areas.

e. Fluorescence Acquisition with inverted view microscope ZEISS

FUCCI cells images will be acquired with the inverted view microscope Zeiss. The laser wavelength for the mKO2-CDT1 channel, and mAG-Gemini channel, are respectively 551 and 492 nm.

III. Results

1. Cell synchronization

In order to synchronize RWPE-1 and PC3-GFP cells in G0/G1 phase, we used the serum deprivation technique, and control our results with flow cytometry. Serum deprivation doesn't

involve any drug, and doesn't alternate the cytoskeleton. Moreover, it is easy to perform, so naturally, this is the first strategy we decided to test.

In figure 1a and 1b, there are the quantitative distributions of the RWPE-1 cells in serum deprivation and control condition, after FACS analysis. The proportion of cells in G1, S and G2/M is almost the same in both conditions. We can conclude that the 24 hours serum deprivation did not work on RWPE-1 cells to synchronize them in G0/G1

We can see for the PC3-GFP serum deprivation on figure 2, that we have an enrichment of almost 20 % of the phase G1/S in absence of serum, compared to the control condition. The serum deprivation partially worked for the PC3-GFP cells.

2. Comparing cell distribution in the cell cycle phases, with the mechanical subclasses' proportions

However, we can compare the RWPE-1 (figure 1a) and PC3-GFP (figure 2) distribution in the cell cycle, with the mechanical subclasses' proportions, obtained during previous work of the team, after unsupervised machine learning analysis (figure 3 and 4b).

Concerning the RWPE-1 cells, we can see the cell cycle distribution in figure 1a and subclass proportions in figure 3. In both cases, the cells are divided into 3 categories, with one main category and two secondary categories. But the different proportions between the distribution of cells in the cell cycle, and the subclasses proportions, do not really correspond to each other.

Concerning the PC3-GFP cells, subclass 1 (figure 4b) representing 70 % of the cells, has almost the same proportion as cell distribution in G1/S (figure 2), which is 63.1%. The 3 remaining mechanical subclasses may correspond to cells in S/G2/M. So, the mechanical signature from subclass 1 could correspond to cells in G1/S, and cells in S/G2/M may show the mechanical signature from subclasses 2, 3 and 4.

IV. Discussion

Concerning the cell synchronization using serum deprivation on RWPE-1, there are some hypotheses to determine why it did not work. The serum deprivation time may not be long enough. It would be wise to extend the serum deprivation time: 48 hours instead of 24 hours for example. The factor growth deprivation would be more effective than before. Actually, serum deprivation tests are underway to determine at what point in time there is a difference between cells with and without serum. Moreover, RWPE-1 cell line is a transgenic cell line genetically modified to express immortality genes, which gives cells the ability to divide indefinitely and independently. The lack of growth factors contained in the serum could not be enough to avoid cell cycle progression. The use of drugs that synchronize cells without changing the dynamics of the cytoskeleton may be a good alternative. Aphidicolin, for example, synchronizes cells in phase G1/S by inhibiting DNA polymerase (Jackman *et al.* 2001). Concerning the PC3-GFP cells, we observed an enrichment of the G1/S phase after serum deprivation. But, during the flow cytometry analysis, it was not possible to place a sufficiently precise threshold in order to differentiate the G1 phase from the S phase. So, we don't know if the enriched phase is the G1, S, or both.

For the RWPE-1, the mechanical subclasses could include cells from different phases, but showing the same mechanical signature. For example, subclass 1, which represents 85 % of the cell population, could include all the cells in G1 (65.13 %), and may be cells in early phase S (a portion of 29.35 %). In that case, the proportions and the distributions would match better. To further explore this question, in a future work, it would be wise to do some research concerning the cytoskeleton activity during the early phase S. The cell biomechanical properties in early S could be similar to cells in G1.

Moreover, the fluorescence intensity thresholds used to analyze the flow cytometry results are set manually. They therefore represent a significant bias for the quantification of the distribution in the cell cycle. Therefore, we cannot expect the proportions of the subclasses and the distribution in the cell cycle phases to match perfectly.

FUCCI (Fluorescent Ubiquitination-based Cell Cycle Indicator) cells developed by Sakaue-Sawano *et al.* (2008) are a valuable alternative to serum deprivation for studying the cell cycle. The FUCCI system allows us to visualize the different phases of the cell cycle in real time using fluorescent proteins.

Unlike serum deprivation, which involves removing serum from the cell culture medium to induce cell cycle arrest, FUCCI cells offer a non-invasive and more precise method for tracking cell cycle progression. By combining fluorescent microscopy with AFM, single cell force measurements will be performed knowing if the cell is in G1 (red), early S (yellow), and S/G2/M (green). By this way, the force curves obtained will be compared.

V. Acknowledgments

I had the opportunity to be guided by Ophélie THOMAS-CHEMIN (PhD student), who supported me during my experiments, introduced me to the principles of Atomic Force Microscopy, and shared insights into the potential of this technology. She also generously provided the results of her previous research. Her valuable guidance greatly contributed to the writing of this report. I sincerely thank her for the time she dedicated over the past months and for her warm welcome within the Elia team.

I would like to thank Etienne DAGUE (research director) for his valuable guidance on my work and oral presentations, which has greatly contributed to my progress.

Thanks to Charline Blatche and Doriane Desandré for having respectively trained me in cell culture and bacteriology.

Thank you to all the Elia team for their warm welcome.

VI. References

Cross, S. E.; Jin, Y.-S.; Rao, J.; Gimzewski, J. K. (2007). "Nanomechanical Analysis of Cells from Cancer Patients". Nature Nanotech, 2(12), 780–783. PMID: N/A. DOI: 10.1038/nnano.2007.388.

Hutchinson-Gilford Progeria Syndrome: A Premature Aging Disease. (2017). PMID: 28660486.

Muscular Dystrophy: Disease Mechanisms and Therapies. (2015). PMID: 26380274.

Elasticity, Adhesion, and Tether Extrusion on Breast Cancer Cells Provide a Signature of Their Invasive Potential. (2016). PMID: 27701866.

Visualizing Spatiotemporal Dynamics of Multicellular Cell-Cycle Progression. (2008). PMID: 18267078. DOI: 10.1016/j.cell.2007.12.033.

Mechanical Properties of the Cytoskeleton and Cells. (2017). PMCID: PMC5666633.

Methods for Synchronizing Cells at Specific Stages of the Cell Cycle. (n.d.). DOI: 10.1002/0471143030.cb0803s00.

VII. **Scheme**

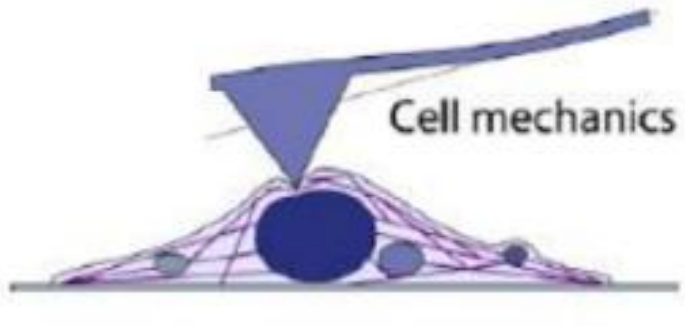

Schema 1: Cell indentation using cantilever to measure biomechanical properties.
Source: JPK instruments nanowizard

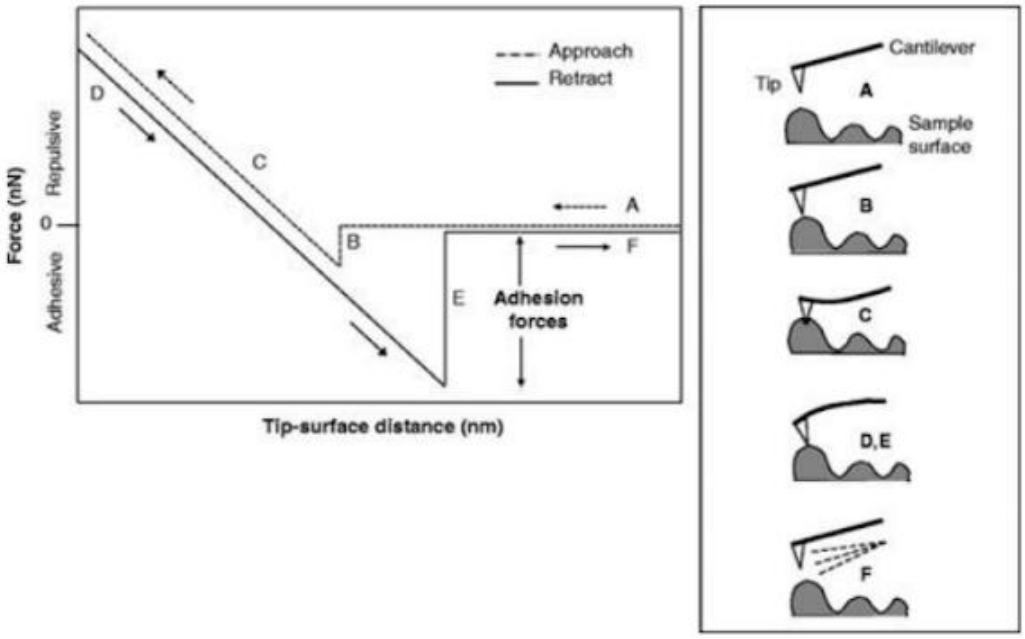

Schema 2: Obtaining Force-distance curve using Atomic Force Microscopy
Source: J Cell Sci (2005) 118 (13) : 2881-2889

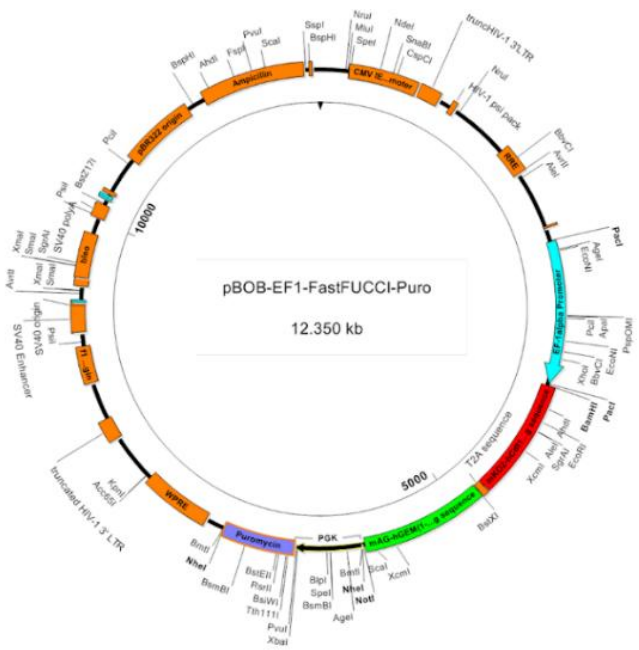

Figure S1, related to Figure 1. pBOB-EF1-FastFUCCI-Puro construct
Full map of the pBOB-EF1-FastFUCCI-Puro construct. See Supplementary Table S1 for all single and two-cutter 6+ nucleotide restriction enzymes with respective positions and actual nucleotide numbers.

Schema 3: Full map of the pBOB-EF1-FastFUCCI-Puro construct
Source: J Cell Sci. 130 :doi :10.1242/jcs.195164 :Supplementary information

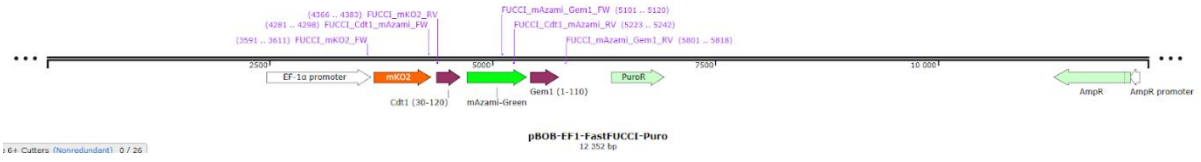

Schema 4: Map of the 3 primers pairs overlapping sequences of interest
Source: Snap gene

VIII. Figures

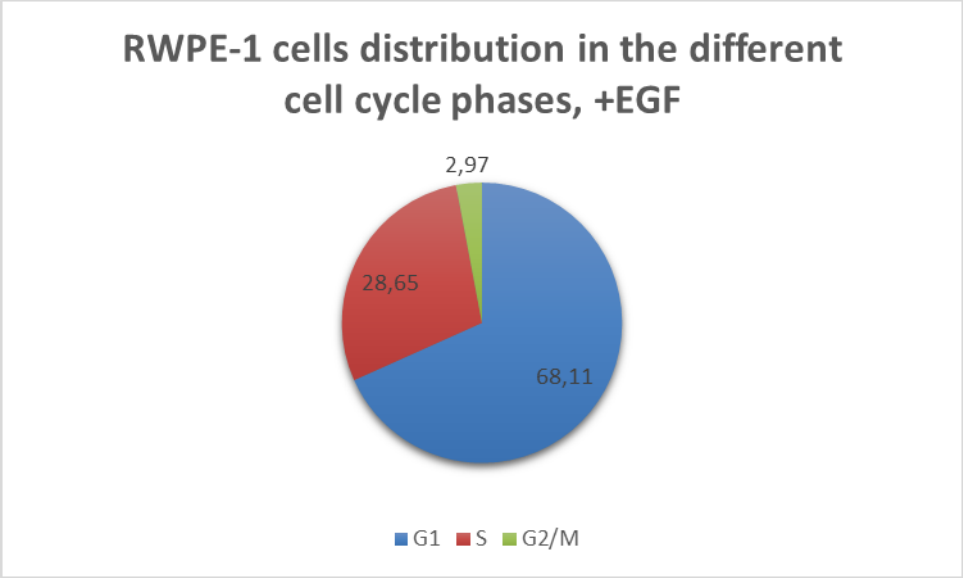

Figure 1a: RWPE-1 cells distribution in the different cell cycle phases in presence of EGF

RWPE-1 cells were cultured in presence of 10 % EGF, stained with Iodure Propidiuim with a concentration of 50 µg/mL and KI-67 antibody diluted at 1/100. Cells were analyzed by FACS.

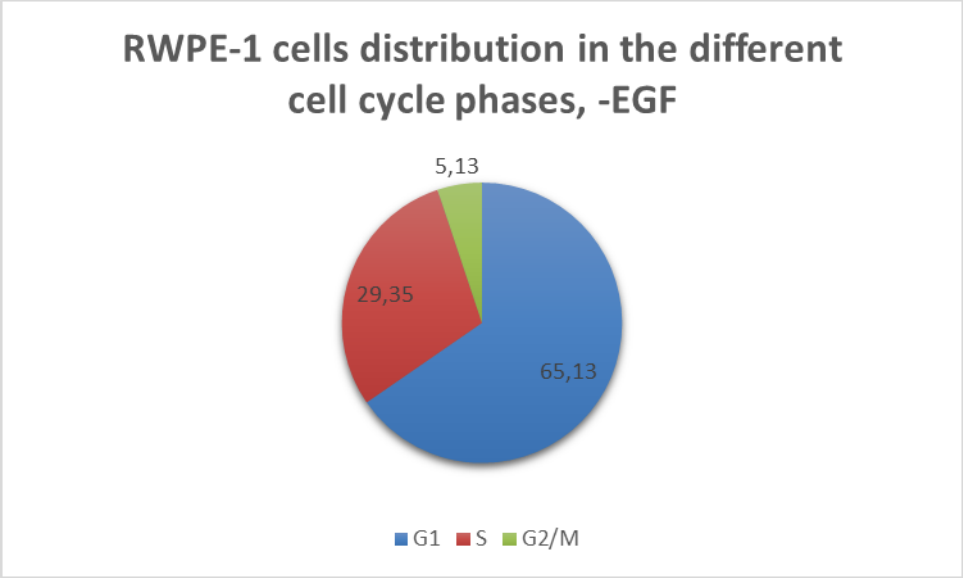

Figure 1b: RWPE-1 cells distribution in the different cell cycle phases without EGF

RWPE-1 cells were cultured in absence of EGF during 24 hours, stained with Iodure Propidiuim with a concentration of 50 µg/mL and KI-67 antibody diluted at 1/100. Cells were analyzed by FACS.

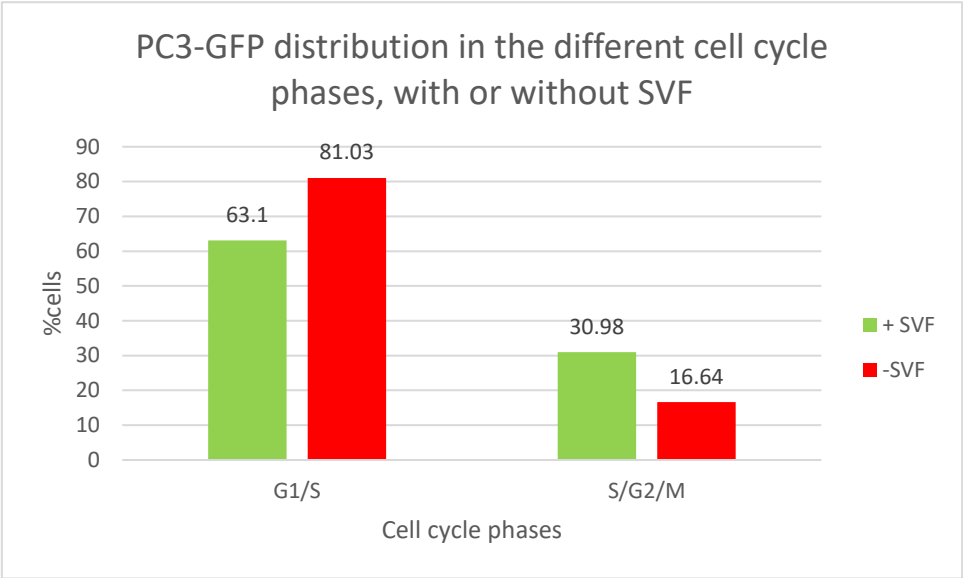

Figure 2: Comparing the PC3-GFP cells distribution in the different cell cycle phases, with or without SVF

PC3-GFP cells were cultured in presence or in absence of 10 % SVF, stained with Iodure Propidiuim with a concentration of 50 µg/mL and KI-67 antibody diluted at 1/100. Cells were analyzed by FACS.

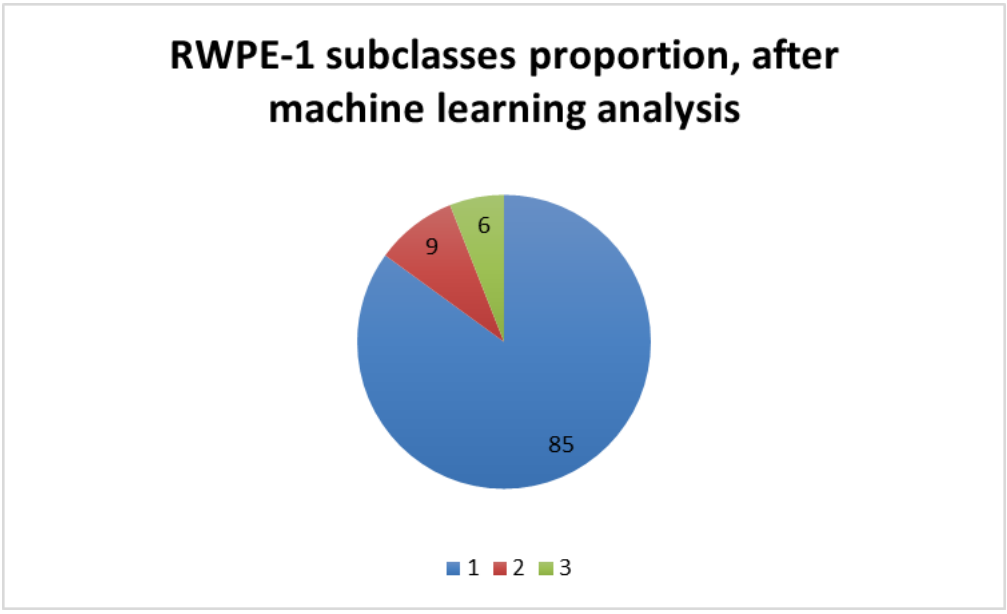

Figure 3: RWPE-1 cells subclasses proportion, after machine learning analysis

Single cell force measurements were performed on RWPE-1 cells cultured in normal condition using NanoWizard® III AFM device. Calibration of the cantilevers (sensitivity and spring constant) have been performed before the acquisition. Force curves analysis were performed using unsupervised machine learning.

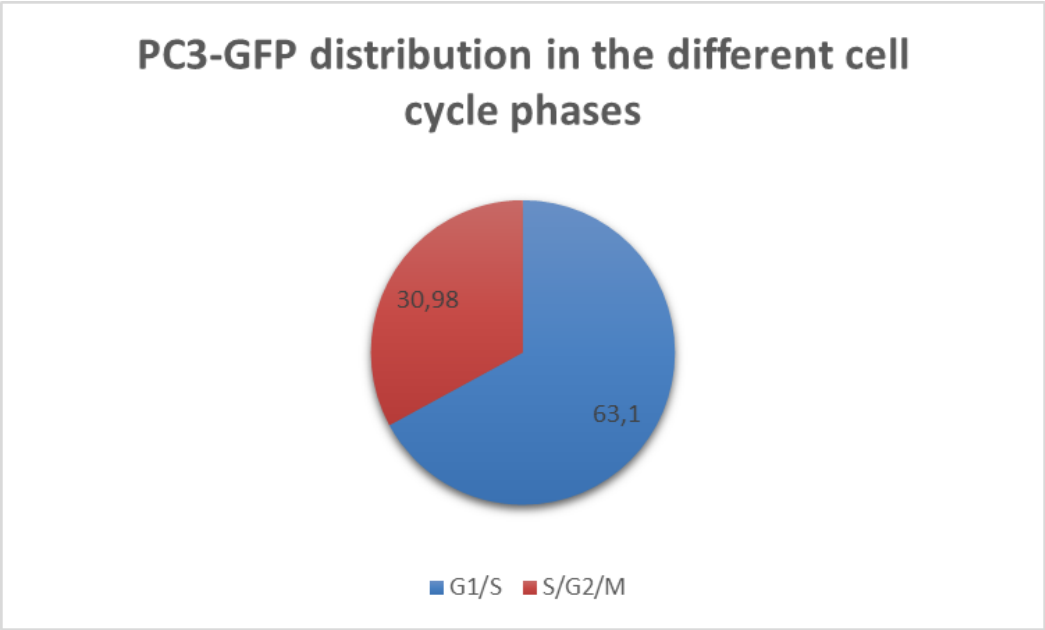

Figure 4: PC3-GFP cells distribution in the different cell cycle phases

PC3-GFP cells were cultured in presence of 10 % SVF, stained with Iodure Propidiuim with a concentration of 50 µg/mL and KI-67 antibody diluted at 1/100. Cells were analyzed by FACS.

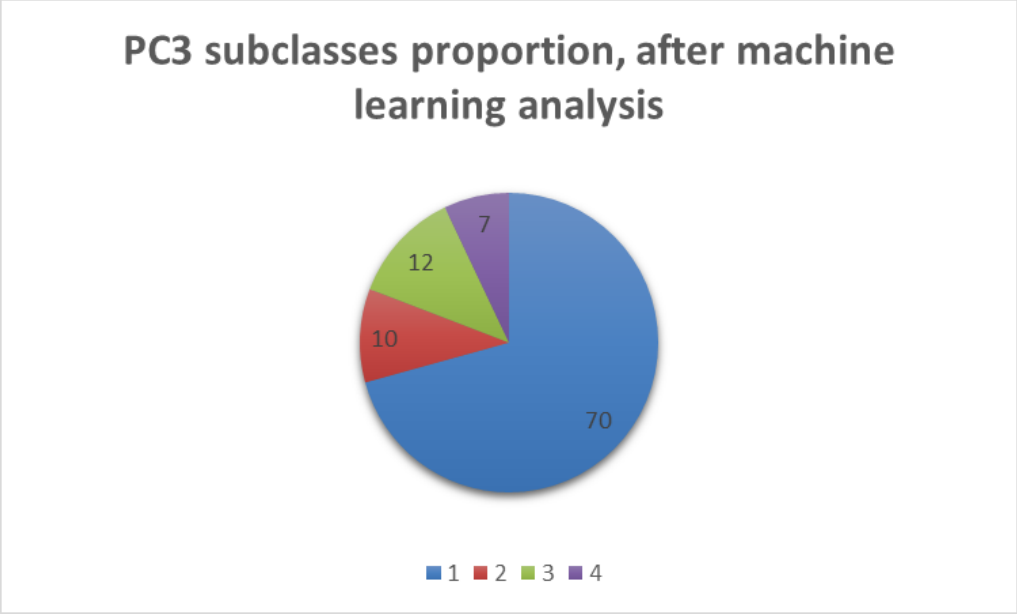

Figure 5: PC3-GFP cells subclasses proportion, after machine learning analysis

Single cell force measurements were performed on PC3-GFP cells cultured in normal condition using NanoWizard® III AFM device. Calibration of the cantilevers (sensitivity and spring constant) have been performed before the acquisition. Force curves analysis were performed using unsupervised machine learning.